Chapter 9
Compliant Mechanisms in Plants and Architecture

Simon Poppinga, Axel Körner, Renate Sachse, Larissa Born, Anna Westermeier, Linnea Hesse, Jan Knippers, Manfred Bischoff, Götz T. Gresser, and Thomas Speck

Abstract Plant movements can inspire deployable systems for architectural purposes which can be regarded as ideal solutions combining resilient bio-inspired functionality with elegant natural motion. Here, we first give a concise overview of various compliant mechanisms existing in technics and in plants. Then we describe two case studies from our current joint research project among biologists, architects, construction engineers and materials scientists where the aesthetic movements of such role models from the plant kingdom are analysed, abstracted and implemented in bioinspired technical structures for sustainable architecture. Both examples are based on fast snapping movements of traps of carnivorous plants. The Waterwheel plant (*Aldrovanda vesiculosa*) captures prey underwater and the Venus flytrap (*Dionaea muscipula*) snaps in the air. We present results on the motion principles gained by quantitative biomechanical and functional-morphological analyses as well as their simulation and abstraction by using e.g. Finite Element Methods. The

S. Poppinga (✉) • L. Hesse
Plant Biomechanics Group, Botanic Garden, Faculty of Biology, University of Freiburg, Schänzlestraße 1, D-79104 Freiburg, Germany
e-mail: simon.poppinga@biologie.uni-freiburg.de

A. Körner • J. Knippers
Institute of Building Structures and Structural Design (ITKE), University of Stuttgart, Keplerstraße 11, 70174 Stuttgart, Germany

R. Sachse • M. Bischoff
Institute for Structural Mechanics (IBB), University of Stuttgart, Pfaffenwaldring 7, 70550 Stuttgart, Germany

L. Born • G.T. Gresser
Institute for Textile Technology, Fiber Based Materials and Textile Machinery (ITFT), University of Stuttgart, Pfaffenwaldring 9, 70569 Stuttgart, Germany

A. Westermeier • T. Speck
Plant Biomechanics Group, Botanic Garden, Faculty of Biology, University of Freiburg, Schänzlestraße 1, D-79104 Freiburg, Germany

Freiburg Centre for Interactive Materials and Bioinspired Technologies (FIT), University of Freiburg, Georges-Köhler-Allee 105, D-79110 Freiburg, Germany

J. Knippers et al. (eds.), *Biomimetic Research for Architecture and Building Construction*, Biologically-Inspired Systems 9, DOI 10.1007/978-3-319-46374-2_9

Aldrovanda mechanism was successfully translated into a similarly aesthetic and functional technical structure, named Flectofold, which exists in a prototype state. The Flectofold can be used as a façade shading element for complex curved surfaces as existing in modern architecture.

9.1 Introduction

Compliant mechanisms are omnipresent in nature and, until now, have mostly been used for small technical devices, e.g. in the medical or packaging industries or in microelectromechanical systems (MEMS) but are widely unknown on the larger scale of building construction (Howell 2001). The urgent demand for more energy-efficient and sustainable architecture has led to a growing interest in adaptive building envelopes that can adjust themselves to changing external environmental conditions or internal comfort requirements. For kinetic systems in building construction, the criteria of "robustness" and "adaptability" are usually of major importance, whereas other aspects such as "accuracy" or "velocity" are of less relevance (Knippers and Speck 2012; Speck et al. 2015). Movements of many plant surfaces fulfil these criteria and are additionally interesting because of their often highly aesthetic movement patterns (Speck 2015). Petals and leaves do not only rotate around static axes (as it is the case in technical motions) but perform more complex, three-dimensional movement patterns based on countless robust principles important for many vital functions. These movements are based on the locally adapted stiffness of their components and avoid high stress and strain concentrations. An important issue for quantitatively understanding and describing these movements and for the transfer into bio-inspired technical solutions is the elucidation of movement patterns and of actuation principles and their interplay with the structural set-up of the mechanism because geometrical characteristics and material parameters are inseparably linked and similarly affect the motion behaviour of the compliant mechanism. In addition to quantitative studies of the biomechanics of plant movements and of the underlying structures, simulations of the movement and of the actuation mechanisms with kinetic FE models render especially valuable contributions for such analyses (Poppinga et al. 2013; Schleicher et al. 2015). A combination of these methodological approaches is not only mandatory for successful biomimetic transfer, but also facilitates an improved understanding of the biological role models in the process of reverse biomimetics (Speck and Speck 2008).

Despite an increasingly better comprehension of the functional aspects of the movements of plants since the appearance of the classic works of Charles Darwin (Darwin 1865, 1875), many questions concerning form-structure-function relationships remain to be solved, which, in addition to their biological interest, are also of great importance for successful transfer into biomimetic products. The idea that plant movements represent suitable role models for bio-inspired adaptive building envelopes has been established by the development and patenting (Knippers et al. 2011) of the biomimetic façade-shading system Flectofin®, which

is composed of laminated glass-fibre reinforced polymers (GFRP). This case study covers the flapping mechanism inspired by the deformation principle found during the pollinator-induced deformation of the "perch" of the bird-of-paradise flower (*Strelitzia reginae*) (Lienhard et al. 2011; Knippers et al. 2012; Speck et al. 2015). Based on experiences with this successful biomimetic invention, further studies of selected especially promising biological role models, namely the Venus flytrap (*Dionaea muscipula*) and Waterwheel plant (*Aldrovanda vesiculosa*), have been performed and new biomimetic façade-shading systems have been and are currently being developed.

9.2 A Comparison of Technical Hinges and Flexible Joints in Plants

Deployability in technical constructions is typically achieved by joining stiff elements that have the ability to glide against each other (rigid-body mechanisms) (Howell 2001). With respect to adaptive building envelopes, Velasco et al. (2015) have classified certain types of mechanisms that are used in construction today and discerned, for example, deployable structures (folding grills, telescopic, tensegrity and tension structures, folding plates and pneumatic systems), various types of physical transformations (deformation, folding, deploying, retraction, sliding and revolving) and the involved direction of movements (spherical movement, circular tangential movement, radial movement, pivoting movement, monoaxial movement, biaxial movement and multiaxial movement). Most of the adaptive building systems such as façade-shading systems rely on rigid or membranous elements guided along linear and parallel translation axes or linear rotation axes, manufactured as standardised elements. This construction principle allows, in many cases, cheap and simple setups but the resulting structures also have the disadvantages of wear, backlash, high numbers of component parts and, hence, assembly costs and expenditure of time (amongst others). Furthermore, their adaptability to non-planar building geometries is limited. In contrast, compliant mechanisms show deployability because of their elastic deformation and rely on the flexibility of their components. Such mechanisms can be completely free of typical joints; hence, markedly reduced maintenance is needed and the whole structure can be constructed in a much lighter and less complex manner, as the amount of structural components (fasteners, springs, etc.) is greatly reduced.

As plant cells possess stiff cell walls (Burgert 2006), the implementation of contractile proteins, which are the basis for muscle-generated movement found in animals, is impeded. Therefore, plants cannot install "motors" for the actuation of rigid-body mechanisms but have instead evolved a multitude of flexible movement principles. Classically, one distinguishes between nastic motions, which follow morphologically predetermined movement patterns, and tropisms, which do not follow such patterns but are determined in movement direction and pattern by

a stimulus. Nastic motions show a clear structure-function relationship and are therefore extremely interesting for biomimetic approaches (Burgert and Fratzl 2009). On the other hand, tropisms display a higher adaptability of the performed motions in terms of possible structural deformation as a reaction to triggering stimuli. Plant motions can be actuated hydraulically, which involves the swelling and shrinking processes of cells and tissues, and/or rely on a release of stored elastic energy (Skotheim and Mahadevan 2005; Forterre 2013). Both principles can be reversible (turgor change in cells, elastic organ deformation) or irreversible (growth, explosive fracture). Moreover, completely passive movements occur that are actuated by external mechanical forces, e.g. the pushing force or the body weight of pollinators (Skead 1975; Reith et al. 2006).

To our best knowledge, no analogues of rigid-body mechanisms exist in the plant kingdom, other than in fungi. The fruit bodies of *Macrolepiota* species (Agaricaceae), for example, are characterised by movable rings (annuli) around the respective stipes (cf. Ge et al. 2010) (Fig. 9.1a). During development of the fruit body, the cap-stipe-connection zone breaks because of cap expansion, leaving the ring, which behaves similar to an uniaxially moving prismatic joint thereby providing a linear sliding movement between two rigid bodies (one degree of freedom). The function of this remarkable structural feature remains to be investigated.

9.2.1 Mechanisms with Concentrated Compliance

Mechanisms with concentrated compliance ("lumped compliance") are characterised by the localisation of elastic deformation, during motion, only to a small structural component and not of the whole structure (Howell 2001). Such mechanisms behave similar to rigid-body mechanisms, but with the rigid hinge being replaced by a flexural joint. Small flexural hinges are sometimes referred to as "living hinges" when they consist of the same material as the two rigid parts that they connect. In plants, movability is often enabled by narrow/thin structures that allow motion of a "rigid" organ connected to a "rigid" plant body. For example, the pulvinus is the typical small joint of an actively moving leaf and functions via osmotically driven swelling and shrinking processes of antagonistically working motor cells (reviewed by Braam 2005; Dumais and Forterre 2012; Poppinga et al. 2013). In some plants, e.g. the nyctinastic silk tree (*Albizzia* spp.) and the thigmonastic sensitive mimosa (*Mimosa pudica*) (Fig. 9.1b), the pulvinus allows for a downwards and upwards bending of leaves (Weintraub 1952; Campbell and Garber 1980) and, hence, resembles a technical hinge joint with one degree of freedom.

Another uniaxially movable plant hinge, which instead works in a completely passive manner, is present in the flower lip (labellum) of the deceptive *Drakaea* orchid (Fig. 9.1c). Male wasps are attracted by the lip, which resembles a flightless

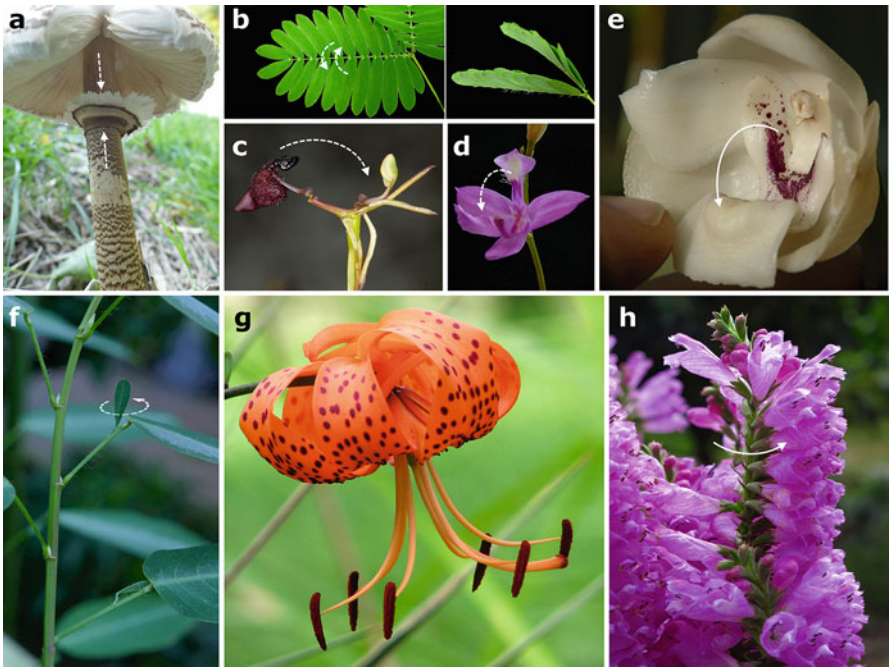

Fig. 9.1 Rigid-body-mechanism in fungi and mechanisms with concentrated compliance in the plant kingdom. Possible movement directions are indicated by dotted arrows, whereas previously performed motions are indicated by arrows with continuous lines. (**a**) The fruit body of *Macrolepiota* spec. is characterised by a movable ring (annulus) around the stipe. (**b**) The sensitive Mimosa (*Mimosa pudica*) folds its leaflets as a response to touch. Moreover uniaxial but, instead, completely passive motions are performed by the hinged labellae of the orchids (**c**) *Drakaea glyptodon* (image with kind permission from photographers Anja and Holger Hennern), (**d**) *Calopogon tuberosus* and (**e**) *Peristeria* spec. (**f**) The leaflets of *Desmodium motorium* move in elliptical circles. (**g**) *Lilium lancefolium* possesses dangling anthers that perform multiaxial passive motion induced by wind and pollinators. (**h**) The flowers of the Obedient plant (*Physostegia virginiana*) can be pushed and rotated in any direction, where they remain. In this image, they have been manually pushed to the right

female, grab the putative copulation partner and try to fly away with it (Peakall 1990). Because of the hinge, the wasp take-off results in an arch-like motion towards the flower and pollination takes place. Although this plant-insect interaction is well-investigated in an ecological context, the detailed functional morphology of the hinge, which allows the violent pollination/attempted copulation action, is still unknown. In other orchids, e.g. *Calopogon tuberosus* (Fig. 9.1d) and *Peristeria spec*. (Fig. 9.1e), the uniaxially movable labellum also aids in pollinator positioning (van der Cingel 2001) and the comparably large hinge lies along a strip-like connection line. A similar hinge mechanism is found in the staminal levers of sages (*Salvia* spp.) and secures pollen deposition on specific regions of the pollinator body (Reith et al. 2006, 2007).

Other plants possess hinged anthers or leaflets that can perform even more complex multiaxial motion, resembling technical structures with ball and socket joints with two degrees of freedom. The leaflets of the Telegraph plant (*Desmodium motorium*) (Fig. 9.1f), for example, perform ultradian motions in elliptical circles every few minutes (Antkowiak et al. 1991). The dangling anthers of *Lilium lancefolium* (Liliaceae) (Fig. 9.1g) help in stripping off the pollen onto the body of the pollinator. This noticeable anther flexibility is often initiated by the dehydration of the filament tip (Keijzer et al. 1987). Indeed, small, thin and, at the same time, flexible and mechanically resilient structures often enable organ deployability in the plant kingdom.

A special case is the movable flower of the Obedient plant (*Physostegia virginiana*) (Fig. 9.1h). The flower is connected to the plant body by a short stalk, which enables a movability that is, to our best knowledge, unique in the plant kingdom. The flower can be pushed and rotated in any direction, where it remains. This is in contrast to other passive plant motions whereby the organs flip back to their original position once the deflecting force stops acting. This hinge type can be compared with a lockable technical ball joint with three degrees of freedom. The biological meaning for this high movability and adaptive stiffness of the flower stalk remains unclear. Müller (1933) identified highly extensible cells that occur in a so-called twisting zone ("Drehzone") and that probably induce the observed flexibility.

9.2.2 Mechanisms with Distributed Compliance

A flexible structure that deforms over its entirety and not only at small flexible joints is considered to have a mechanism with distributed compliance. During the motion, stresses are not concentrated in small areas but are, rather, distributed over the whole body. Such a mechanism can be found in a multitude of moving plant organs that do not possess localised hinges.

Many uniaxial upwards and downwards bending motions are performed by the respective whole organs. For example, the seed scales of pine cones bend as passive reactions to changes in air humidity. This motion is based on the anisotropic swelling and/or shrinking processes of various cellular tissues (Dawson et al. 1997; Poppinga et al. 2013). Hence, the scale reacts similar to a bimetallic strip but responds to a change in humidity and not to heat. By this means, the whole pine cone opens when it is dry, enabling seed release, and closes into a protective state when it is wet (Fig. 9.2a). Multiaxial bending of entire rod-like structures is represented by the prey-induced bending motions of tentacles in carnivorous sundew plants (*Drosera* spp.) (Fig. 9.2b) (Williams and Pickard 1979).

Other cases of uniaxial motions are present in extendable/retractable plant structures. In horsetails (*Equisetum spec.*) (Fig. 9.2c) and bamboo (e.g. *Dendrocalamus giganteus*), growth and culm elongation can be compared with the extension of a tapering telescope (Niklas 1992). Interestingly, plants show a multitude of structures that can be regarded as an analogue to a technical spring, such as the cucumber

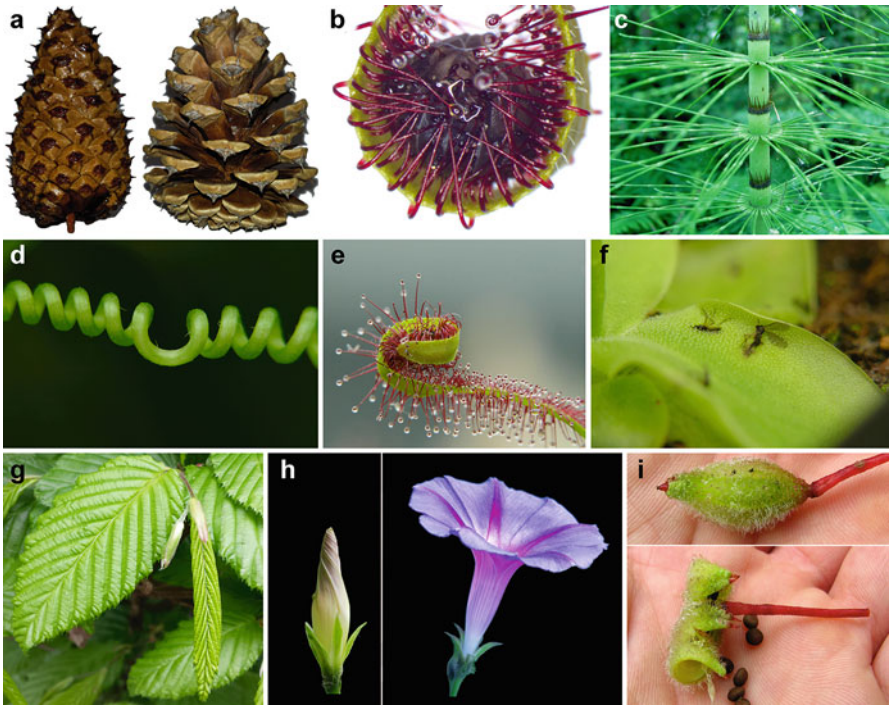

Fig. 9.2 Examples of mechanisms with distributed compliance from the plant kingdom. (**a**) A pine cone in the wet and closed (*left*) state and in the dry and open (*right*) state. (**b**) Sticky tentacles of the carnivorous Cape sundew (*Drosera capensis*) are bent towards captured prey. (**c**) Horsetail culms (shown: *Equisetum telmateia*) elongate by a telescope bar-like movement. (**d**) The Red bryony (*Bryonia dioica*) tendril is a natural spring featuring a reversal in its rotating direction. (**e**) Tropistic motions such as the leaf movement in the carnivorous Cape sundew (*Drosera capensis*) and (**f**) in butterwort leaves (*Pinguicula grandiflora*) around caught prey are complex mechanical responses depending on the direction of the triggering stimuli. (**g**) Processes of leaf unfolding in the European hornbeam (*Carpinus betulus*) follow a complicated origami pattern and (**h**) the opening movements of sympetalous flowers (*Ipomoea purpurea*) are important ontogenetic processes. (**i**) Explosive fracture of Touch-me-not (*Impatiens balsamina*) fruits

tendril (Fig. 9.2d) (Gerbode et al. 2012), which shows structural adaptations for strain-stiffening and for avoiding unwinding under tension. Even more complex three-dimensional motions of planar surfaces are performed by the sticky leaves of carnivorous sundews (Nakamura et al. 2013). Upon contact with caught prey, bending motions lead to the wrapping of the leaf around the animal and the formation of an "outer stomach" (Darwin 1875) (Fig. 9.2e). Similar motions are performed in butterworts (*Pinguicula* spp.) by their planar adhesive trapping leaves (Heslop-Harrison 1970), which either wrap around the prey or form depressions on their leaf surfaces for deterring escape (Fig. 9.2f). Mechanisms with distributed compliance also play a crucial role in many ontogenetic processes, for example, in unfolding leaves, which can follow a complex origami pattern (Kobayashi et al.

1998) (Fig. 9.2g) or in blooming processes of flowers (Liang and Mahadevan 2011; van Doorn and van Meeteren 2003; van Doorn and Kamdee 2014) (Fig. 9.2h).

Some plant organs change their shape very rapidly. The explosive bursting of fruits, e.g. in Touch-me-nots (*Impatiens* spp.) (Deegan 2012) (Fig. 9.2i), is irreversible because the whole structure is torn. Fast and reversible motions often rely on snap-buckling (snap-through) processes of doubly-curved shell-like structures. Because of the double curvature, tension and compression stresses occur when the organ is deformed and elastic energy is stored and eventually released when the curvature suddenly inverts. Hence, plant organs incorporating such elastic components first build up and store elastic energy by either passively or actively deforming a doubly-curved organ and achieve a very rapid and strong passive mechanical response. This movement principle is scalable and can be found in minute spores of eusporangiate ferns (diameter: 30 μm) (Hovenkamp et al. 2009), in ca. 500 μm long trapdoors of carnivorous bladderwort traps (*Utricularia* spp.) (Vincent et al. 2011; Poppinga et al. 2016a) and in up to 5 cm long snap traps of the Venus flytrap (*Dionaea muscipula*) (Forterre et al. 2005; Poppinga et al. 2013), which are described in detail in Sect. 9.3.2. Notably, some doubly-curved plant structures such as the false indusia of the Peruvian maidenhair fern (*Adiantum peruvianum*) (Poppinga et al. 2015) invert their curvature without performing a rapid snap-through transition; the underlying mechanism of this action remains to be investigated in detail.

9.3 Biological Role Models

*9.3.1 The Snap-Trap of the Waterwheel Plant (*Aldrovanda vesiculosa)

The aquatic carnivorous Waterwheel plant (*Aldrovanda vesiculosa*), which is distributed almost worldwide, possesses snap-traps typically 2.5–6 mm in length (Cross 2012) (Fig. 9.3) and captures small zooplankton prey. The trap is divided into two lobes that are connected by a midrib. Inside the trap and near to the midrib, several trigger hairs are located that are sensitive to touch by the prey. After being triggered, the fast trap closure lasts 100 ms (Poppinga and Joyeux 2011). Early investigations by Ashida (1934) showed that the trap lobe curvature does not change between the open and closed state but that the midrib curvature alters from straight (open trap) to strongly bent (closed trap). Much later, with the help of high-speed cinematography and computer-based mechanical modelling techniques, Poppinga and Joyeux (2011) were able to show that Ashida's observations are consistent with a trap closure mechanism that is markedly different from that of *Dionaea* (see Sect. 9.3.2). After being triggered by prey, volume changes attributable to turgor losses occur in motor cells situated next to the trap midrib (Ashida 1934), coupled to a bending of the midrib and movement of the lobes towards each other (Poppinga

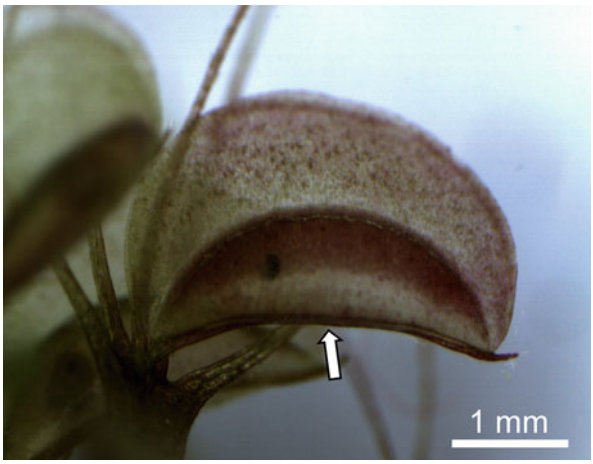

Fig. 9.3 A closed *Aldrovanda vesiculosa* trap. Note the bent midrib (*arrow*)

and Joyeux 2011; Schleicher et al. 2015) (Fig. 9.3). A minute bending of the midrib suffices to initiate trap closure because of kinematic amplification deriving from the trap built-up.

The *Aldovanda* trap can be considered as an example of a mechanism with concentrated compliance (see Sect. 9.2). With the help of modern construction methods, we aim at implementing the *Aldrovanda* kinematic as a feature for inducing deployability in architecture, especially in façade elements for adaptive shading (see Sect. 9.5.1).

9.3.2 *The Snap-Trap of the Venus Flytrap (*Dionaea muscipula)

The *Dionaea* leaf is constituted of a flat petiolus and a leaf blade transformed into the (in)famous snap-trap, which is typically 2 cm in length (Bailey and McPherson 2012). Three trigger hairs sensitive to mechanical perturbations are situated on each of the two trap lobes. Several stimuli by prey (typically crawling arthropods) within a certain period of time are required for the trap to close (duration 0.3 s) (Forterre et al. 2005; Poppinga et al. 2016b). The rapid closure of the traps has fascinated scientists since Darwin's comprehensive works on carnivorous plants (Darwin 1875) and the mechanism by which they do so is still under debate. Active hydraulic processes at the cellular level are commonly accepted to drive the comparably slow first stage of the movement, although the exact mechanism remains to be elucidated. Either active changes in turgor pressure in cells of motor tissue or cell-wall loosening leading to an acid growth response drive this initial motion (Williams and Bennett 1982). Furthermore, the relaxation of pre-stressed tissue(s) has not been ruled out as supporting this process (Hodick and Sievers 1989; Colombani and Forterre 2011).

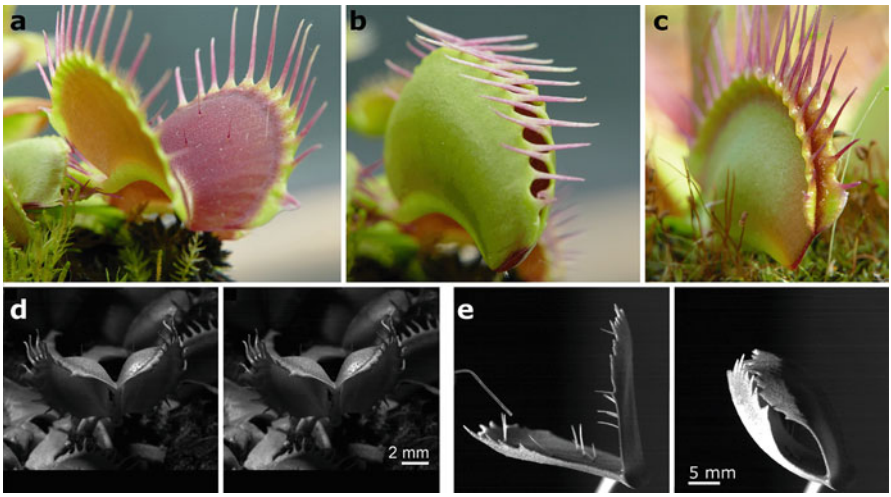

Fig. 9.4 The Venus flytrap wild type and two morphologically divergent cultivars used for investigation of the morphospace of functional (fast) snap-traps. (**a**) An open trap of a wild type plant. Note that the lobes are concave (as seen from the outside) when the trap is open and (**b**) convex when the trap is shut. Small prey can escape through the mesh of "teeth" protruding from the lobe margins. (**c**) Large prey, which cannot escape, triggers complete trap shutting and digestion. (**d**) The cultivar "Angel Wings" possesses trap lobes with extremely strong curvature and these do not shut after triggering (*right image*). (**e**) The cultivar "Korean Melody Shark" possesses trap lobes with little initial curvature and these shut very slowly

This initial motion leads to the deformation of the double-curved lobes, which are initially concave as seen from the outside. As described in Sect. 9.2, elastic energy is stored in the lobes and is released when they flip to a convex curvature (Fig. 9.4a, b). The trap snaps shut and the prey is caught. Hence, the *Dionaea* trap consists of two independent kinematical elements (the two independently, hydraulically and elastically moving lobes) and a midrib that does not actively take part in the motion. In contrast, the previously mentioned *Aldrovanda* trap comprises only one kinematic element (the midrib) whose bending deformation is coupled with lobe movement (see Sect. 9.3.1) (Poppinga et al. 2016b). The "teeth" on the closed trap lobe margins of the Venus flytrap interlock in such a manner that small prey unworthy of activating the energy-demanding digestion process can escape. If the prey is too large to escape and, hence, further stimulates the trigger hairs during its escape attempts, the trap closes completely and the digestion process is initiated (Böhm et al. 2016) (Fig. 9.4c). After digestion and nutrient uptake, the trap reopens after a few days by growth processes, hereby avoiding reverse snap-buckling (Poppinga et al. 2016b).

We have investigated various ontogenetic stages (Poppinga et al. 2016b) and diverse stable mutants (cultivars) with regard to their movement patterns during trap closing. The cultivars are characterised by different morphological variations in the trap form and structure, which hinders (fast) trap closure to a variable

degree. By quantitatively analysing and simulating kinematics of the trap-closing motion of the diverse mutants, we aim to characterise a "morphospace" representing the morphological limits for successful trap action. In addition to an improved understanding of the biological structures and of the structural constraints that have to be fulfilled during trap evolution, this morphospace will also help to define the possible degrees of freedom in shape finding for biomimetic flapping systems inspired by the snap-buckling mechanism of the Venus flytrap.

Our first investigations dealt with the cultivars "Angel Wings" with its conspicuously more strongly curved traps (Fig. 9.4d) and "Korean Melody Shark", which is characterised by an apparent weak curvature of the lobes (Fig. 9.4e) compared with the wild type (Fig. 9.4a). By choosing the two "extremes" in terms of trap-lobe curvature, initial results concerning the possible boundaries of the snap-buckling morphospace could be gained. We performed 3D-scans with a laserscanner (DAVID-SLS-1 structured light 3D scanning, DAVID Vision Systems GmbH, Koblenz) of open and closed traps and recorded the respective, manually triggered motions with a high-speed camera (Motion Pro Y4, IDT, Tallahassee, USA, recording speed 1000 fps). We have found that the trap motion in the cultivar "Angel Wings" is blocked shortly after triggering. Because of the strong lobe curvature, the energy barrier between the concave and convex lobe states is apparently so high that pure hydraulics are not sufficient to cause trap closure. By manually pressing the trap lobes together, they can be brought into a closed state. On the contrary, in the trap of the cultivar "Korean Melody Shark", we have observed a slow and continuous motion (snapping duration: 2.2 s). Here, the lobe curvature and, consequently, the elastic instability is much less pronounced compared with the wild type. Hence, we hypothesize that little elastic energy can be stored and released during trap motion. The motion in a wild type trap shows a characteristic sequence of motion steps of highly different speeds (slow initial motion, fast snap-buckling, slow final closure) (cf. Forterre et al. 2005; Poppinga et al. 2016b). Assuming that the lobe anatomy and the physiology behind the hydraulic movement do not differ in general between the cultivars and the wild type, we speculate that the different trap behaviours (no snapping, normal snapping, slow snapping) can be explained by the different lobe curvatures. This indicates that geometric limitations are indeed present with respect to the mechanics and dynamics of *Dionaea muscipula* traps. A planned extension of the test specimens including cultivars with intermediate lobe curvatures and with trap shapes strongly diverging from the normal bauplan will lead to further insights into the structural requirements for functional snap-traps.

9.4 Simulation

Mechanical modelling of biological role models aims to provide a deeper understanding of their motion principles and may thus contribute to the field of reverse biomimetics. The Finite Element Method (FEM) provides new possibilities in quantifying the various parameters that have a significant influence on the overall

deformation mechanism. Even though some information about material and geometry and the effect of the environment may still be lacking, assumptions can be made that allow the qualitative simulation of the principal mechanism.

Moreover, various simulation techniques enable the discovered kinetic mechanisms and involved geometrical principles to be abstracted, following the methodology of Schleicher et al. (2015). The process of modelling and simulating mechanisms is divided into three main categories. 1. The geometric model provides a parameterised representation of the underlying geometrical features responsible for the movements. It allows the development of topologically identical variations. 2. The kinematic model is used qualitatively to evaluate the way that the geometric parameters influence the actual movement. 3. Finite element analysis used in the kinetic model permits not only the evaluation of the geometric variations, but also the determination of the manner in which certain material distributions and stiffness gradients influence the energy needed and the related forces therein.

9.4.1 *Simulation of the* Aldrovanda *Trap*

The two trap lobes are connected by a midrib and each is divided into two parts differing in thickness and function (Fig. 9.5). The central portion is located next to the midrib and contains the motor zone that active-hydraulically drives the movement. The outer lobe part is composed only of two thin cell layers (Ashida 1934), leading to a (supposed) much smaller stiffness compared with the central portion consisting of three cell layers. The simulation of the trapping movement as a kinetic model, by using FEM, has been performed by Schleicher (2015). As a result, the principal mechanism, as described in Sect. 9.3.1, could be verified. The objective

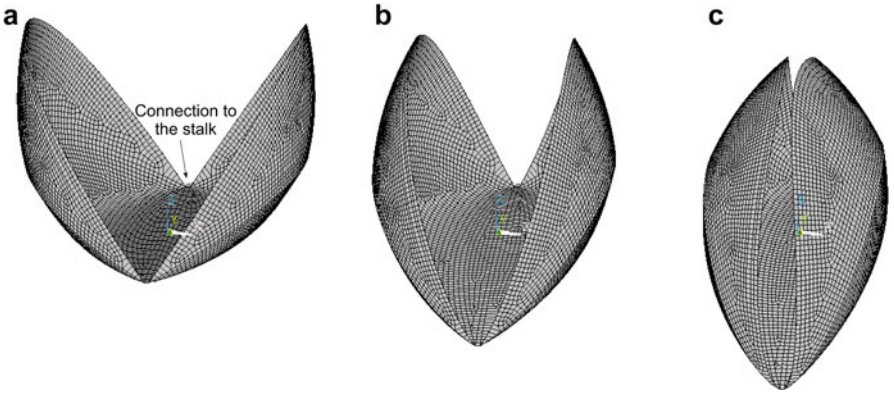

Fig. 9.5 Kinetic model: simulation of the *Aldrovanda vesiculosa* trap with a temperature load case. (**a**) Open state, (**b**) semi-closed state after application of 50 % of the load, (**c**) fully closed state

for future research is to simulate the mechanism in more detail and to quantify important values or limits constraining the closing mechanism. For this purpose, a different finite element model is constructed. Because much of the input data is hard to examine experimentally (e.g. mechanical parameters of tissues), various modelling assumptions for the geometry, material and even load cases need to be made.

Detailed images of the *Aldrovanda* trap from various angles serve as the starting point for the geometry model. The overall dimensions of the geometry match the real size of the trap but the geometric model itself is an idealised one. The base geometry has a midrib length of 6 mm and a width of 4.5 mm, leading to an opening angle of about 70°. The Young's modulus of the lobes is assumed to be 800 N/mm^2 and twice as high for the midrib. Further to emphasis the different levels of stiffness in the zones described in Sect. 9.3.1, thicknesses between 0.03 mm and 0.2 mm are allocated. The displacement boundary conditions are represented by the connection of the midrib to the rest of the leaf. In order to prevent rigid body movements, all degrees of freedom, three translations and three rotations are fixed at one end. To simulate the strain or volume change by turgor variation in the motor cells after trap triggering, a temperature load case is applied to the motor zone. In a geometrically nonlinear analysis of the model, we have found that an isotropic negative temperature load, meaning a contraction of the cells by 11 %, leads to a closure of the trap as illustrated in Fig. 9.5.

Schleicher et al. (2015) have focused on the translation of the trap mechanism into a kinetic curved-line folding model in which two flaps are connected to a stiffer middle part by areas of reduced bending stiffness (Fig. 9.6). The most intriguing aspect for technical use is the extensive amplification of a comparatively small bending deformation of the central part into a large closing movement of the two adjacent flaps. The relationship between bending and opening is determined by the radius of the curved-line fold. To evaluate this correlation, Schleicher et al. (2015) developed a kinematic model by using the "Rigid Origami Simulator" (Tachi 2009), which allows simulation of the folding mechanism of a discretised simplification of the curved-line fold. Although this kinematic model provides an overview of geometrical variations, it lacks precision and the consideration of material properties. Another possibility for approximating the folding behaviour is the method of reflection (Mitani and Iagarshi 2011), which requires that the curved-line fold remains entirely on one plane during the folding process. To simulate the

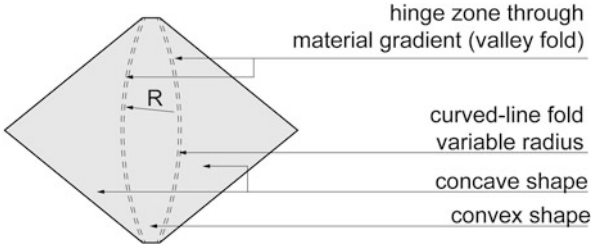

Fig. 9.6 Geometric model: abstracted curved-line folding model

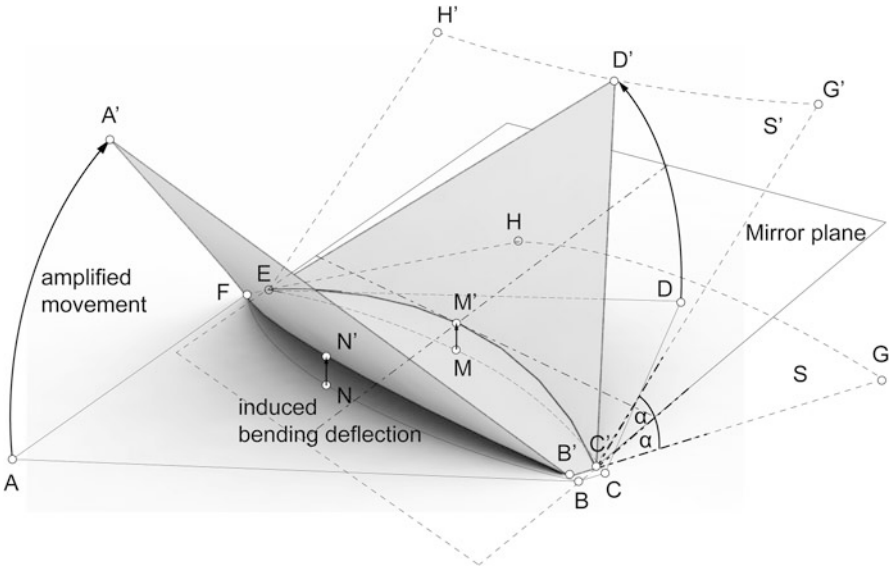

Fig. 9.7 Kinematic model of the abstracted mechanism based on the method of reflection

folding movement, which is controlled by the induced bending, we created a bent midrib geometry in the form of a lens-shaped surface based on the elastica curve in relation to the given translation of control points B and C (Fig. 9.7). The plane given by C′, E and M′ is used to mirror the surface S and the initial outline of the flap surface. Due to the amplification of the folding mechanism only a small translation of B to B′ and C to C′ is needed to result in a complete closure of the component. With the information of curvature and reflected boundary, the folded geometry can be rebuilt. This method not only allows real-time parameter manipulation, but also provides immediate information about the relationship between the displacement of the support points, folding angle and sensitivity of the mechanism and reduces the computational effort compared to spring based methods, especially when it comes to simulations of aggregations of a high number of elements.

The established geometric relationships were transferred into a kinetic model by using FEM software (SOFiSTiK, SOFiSTiK AG, Oberschleißheim, Germany). Several variations regarding the hinge zones in terms of width and stiffness gradient between the hinge, flaps and middle rib have been simulated and evaluated by Schleicher et al. (2015) and Schleicher (2015). When we continued the research with the main focus on the construction of a physical prototype, a rectangular shape with edge lengths of 520 mm and 420 mm was chosen because of the economic production of test objects (see Sect. 9.5.1). Furthermore, the integration of a pneumatic actuator to induce the bending deformation of the central portion was of importance and had to be implemented in the analysis model.

In a first series of digital experiments, an appropriate material gradient between the three zones was established, leading to the desired closing movement. The pneu-

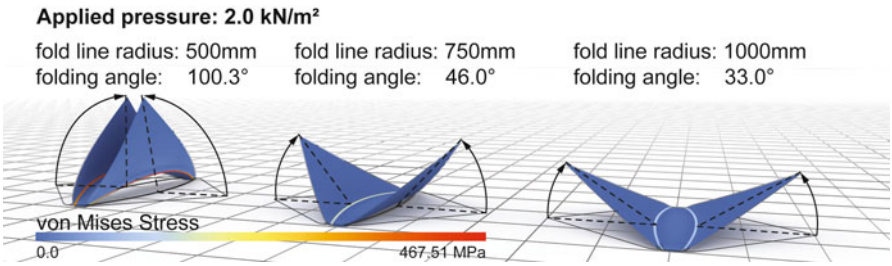

Fig. 9.8 Comparison of models exhibiting various curved-line fold radii to evaluate the required actuation force and corresponding folding movement

matic actuator was simulated by uniformly distributed pressure on the midrib. Even though this does not match accurately a pneumatic cushion, it gives a qualitative insight into the relationship between applied pressure and resultant movement. With this method and the material distribution of a 0.9 mm thick "midrib" and 0.8 mm flaps (Young's Modulus 14000 N/mm^2) and a 0.2 mm thick and 5.0 mm wide hinge zone (Young's Modulus 8000 N/mm^2), a series of different curved-line folds was simulated and evaluated in terms of the required pressure, resultant stresses, corresponding displacement and sensitivity to the actuator (Fig. 9.8). As a summary, it can be stated that a larger radius of the curved-line fold leads to a higher actuation force but less displacement in the midrib. With a smaller radius, the midrib exhibits higher curvature, which is transferred into the flaps, leading to higher geometrical stiffness in the folded position.

For implementation into technical systems, one of the most interesting results in the preliminary research by Schleicher et al. (2015) was the recognition that the basic rectangular shape can be scaled in size and distorted in geometry while remaining operative in these modified instances and boundary conditions. This makes it possible to translate it into various boundary conditions. To keep the movement as consistent as possible between several panels, we developed a method that subdivided a given surface, exhibiting positive and negative Gaussian curvature into adjusted quadrilateral patches of similar anticlastic curvature to ensure a certain pre-fold in the entirely closed condition. The geometric rules of curved-line folding permit the translation of each surface patch into the folded geometry (Fig. 9.9). Further investigations will be addressed to improve the basic geometry in terms of efficiency as shading device, including detailed climatic, physiologic and psychologic comfort studies.

9.4.2 Simulation of the Dionaea *Trap*

Simulation of the *Dionaea* snap-trap makes different demands as it functions with different mechanics than the *Aldrovanda* trap. As mentioned in Sect. 9.3.2, the closure of the *Dionaea* trap can be divided into three phases: a first slow movement

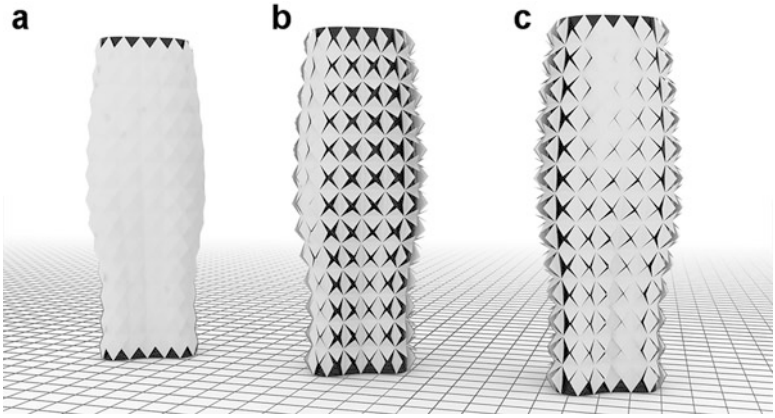

Fig. 9.9 The derived kinetic mechanism is adaptable to geometries of synclastic and anticlastic double curvature. (**a**) Closed postion. (**b** and **c**) Open configurations based on sun vector

driven by hydraulic pressure, a second phase characterised by a high deformation speed during snap-through (also called snap-buckling) and a third slow closing phase. The second process is characterised by a sign change in Gaussian curvature and by the bypassing of an unstable path with negative stiffness.

The geometry of the trap is described by a passive midrib and two active lobes on either side that perform the curvature inversion from convex to concave. These parameters can be directly transferred to a finite element simulation. Because the lobes act independently, in terms of their post-stimulatory movements, and in order to save calculation time, only one lobe is simulated. The geometry is given by a 3D scan that is idealised to a symmetric shape. For the approximate representation of the real cross section, the thicknesses vary between 1 mm at the connection to the midrib and 0.75 mm at the outer end of the lobe. Young's modulus and the Poisson's ratio are assumed to be 1400 N/mm^2 and 0.0, respectively. The boundary conditions can be described by fixing all translations and rotations along the midrib. The measured strain field described by Forterre et al. (2005) has been increased by 50 % and applied as a temperature load case to represent the hydraulic pressure. During a dynamic analysis, this load is gradually increased from zero up to the total load (load factor).

Figure 9.10 shows the load displacement curves of the mid-point of the outer edge of a trap lobe. The movement can be seen to start slowly and represents the change of hydraulic pressure in the initial motion phase. After application of approximately 85 % of the load, snap-through occurs and the deformation speed increases. In contrast to the wild type, the two cultivars behave differently in our simulations according to the different curvature of their lobes. The cultivar "Korean Melody Shark" is characterised by its very weak lobe curvature. The trap

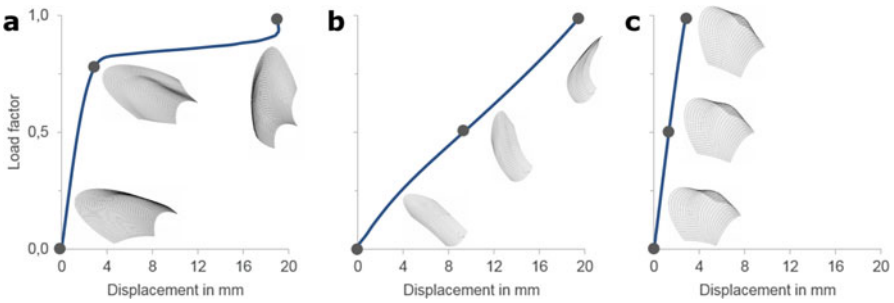

Fig. 9.10 Kinetic models of a Venus flytrap lobe. (**a**) Load-displacement curve and deformation of the normal shaped wild type. Snap-through occurs at 85 % of the load, corresponding to a load factor of 0.85. Load-displacement curve and deformation of the cultivars (**b**) "Korean Melody Shark" and (**c**) "Angel Wings"

closure is a smooth movement without any rapid deformation enhancement. By applying the same load as in the wild type, this behaviour is also visible in the load displacement curve, shown in Fig. 9.10. The opposite of the "Korean Melody Shark" type is presented by "Angel Wings", which exhibits strong curvature of its lobes. The shape of the curve is similar as that for "Korean Melody Shark" but the displacement values indicate that no closure occurs. The applied load is not sufficient to evoke snap-through. These initial simulations generally corroborate the observations described in Sect. 9.3.2.

With regard to technical applications, one of the most noteworthy aspects is the change from a concave to a convex geometry, associated with the bi-stability of open and closed configurations. This change of curvature direction could be advantageous regarding the adaptability to double curved geometries. The transition phase is difficult to control and involves a sudden release of stored elastic energy, which might be problematic for large-scale applications. The investigation of geometrical variations leads to the assumption that the released energy is dependent on the thickness and initial curvature of the lobes (cf. Forterre et al. 2005). Figure 9.11 shows a comparative study based on a parameterised surface with adjustable curvature (Poppinga and Joyeux (2011) and thickness. By using a certain range of expansion (0–0.06 %) uniformly over the whole surface, we can evaluate if and at which expansion rate the snap-through occurs.

To evaluate the influence of stiffness gradients on the released energy, we built a simulation model of about 700 mm/500 mm with constant curvature, actuated by the expansion of a central portion of increased thickness (5 mm, Young's Modulus 14000 N/mm^2). The adjacent surfaces varied in their Young's Moduli (10000 N/mm^2, 7000 N/mm^2 and 4000 N/mm^2) and possessed a thickness of 1 mm. Figure 9.12 shows the initial and deformed shapes and the curvature change along the central axis. The transition is smoother in the case of reduced stiffness of the adjacent surfaces.

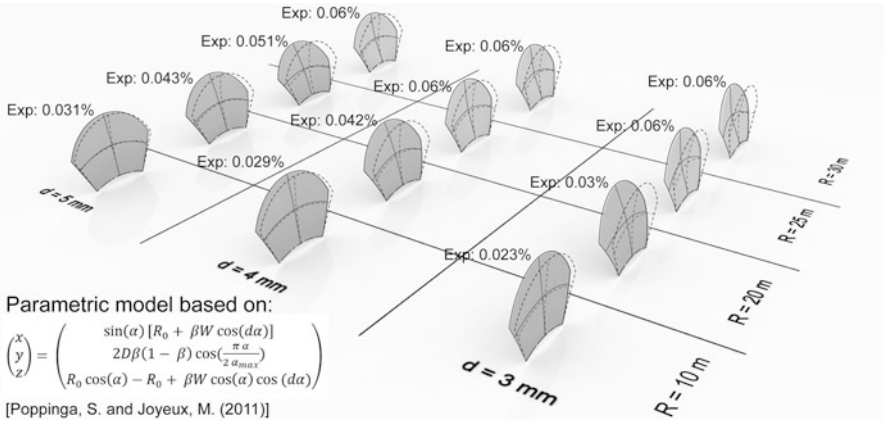

Fig. 9.11 Comparison of the snap-through behaviour of *Dionaea* trap lobe geometries with various initial curvature (based on R in m) and shell thickness (d in mm) with a maximum expansion (Exp) of 0.06 %

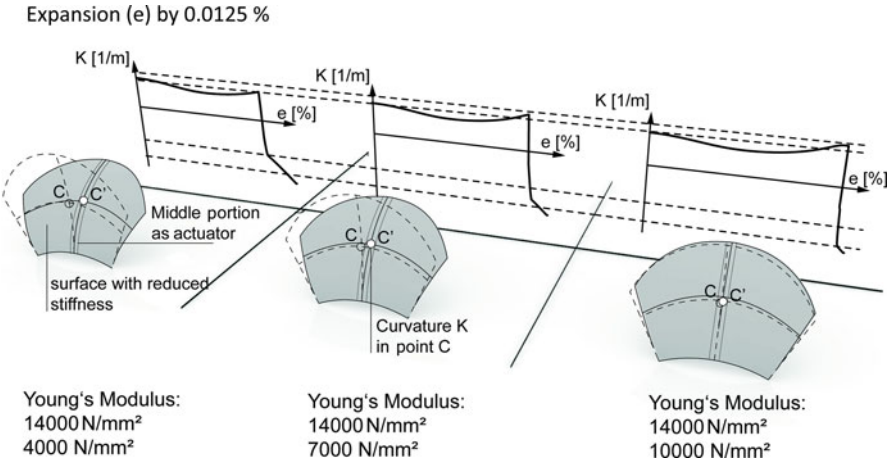

Fig. 9.12 Comparison of the snap-through behaviour of various stiffness gradients between actuator rib and adjacent surfaces. A higher gradient leads to a smoother transition

9.5 Technical Implementation

9.5.1 Technical Implementation of the Trap Movement Principle of Aldrovanda vesiculosa

The technical implementation of the *Aldrovanda* trap movement (Flectofold) is structurally based on defined areas with various mechanical properties. The midrib and the flaps are stiff but remain elastically deformable, while the curved hingezone

(the "technical counterpart" of the elliptical bending zone in *Aldrovanda* trap) is very soft. These areas of the plant with huge differences in the mechanical properties are obtained by precisely defined gradient structures between them. The structure resembles a fibre-reinforced composite with anisotropic and tailored mechanical properties in which the matrix takes the role of load transmission and shaping, whereas the fibres absorb the forces and determine the strength of the component. By using fibre-reinforced plastics (FRP) it was it possible to transfer the structural design of the *Aldrovanda* trap into a first demonstrator and to meet the demanding material requirements in technical applications.

In FRP, mostly stiff fibres are embedded in a shaping matrix to generate tailored mechanical properties that depend on the fibre orientation: a high load-carrying capacity occurs in the fibre direction and a good load-transfer capacity exists perpendicular to the fibre direction (Schürmann 2007). By adaption of i.e. the fibre orientation and the numbers of layers, an anisotropic material can be created. The fibre orientations within one component depend on the textile processes and on the draping of the textile layers onto the form during the fabrication process. In order to obtain various fibre orientations, several textile layers are placed at a certain angle onto each other. Herewith, different fibre orientations can be generated within one component with the aim of defining anisotropic properties and to obtain components with designated bending-zones, i.e. by reduction of the number of textile layers, which are stiff in other zones. These bending-zones are necessary for the implementation of the curved folding principle.

For the technical implementation of curved folding into an FRP component, VAP® (Vacuum Assisted Process) was selected. By using a semipermeable membrane during the vacuum infusion it was possible to reduce air inclusions in the component. Details of this manufacturing process are provided in Henning (2011). During the manufacture of the demonstrator, the resin infusion was applied directly onto a laminating foil (Fig. 9.13), instead of the mould itself. By this means, no preparation of the mould with a release agent is necessary, which makes the process faster and less expensive. Furthermore, the laminating foil is directly integrated into the component in order to avoid potential finishing processes caused by the surface and especially by the colour of the FRP demonstrator.

The material set-up needed for the technical implementation (Fig. 9.13) of the curved folding was determined by a scientific material analysis. The tested resins

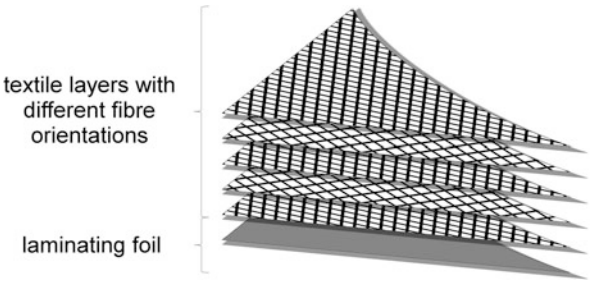

Fig. 9.13 Basic laminate set-up of one shading element of the Flectofold

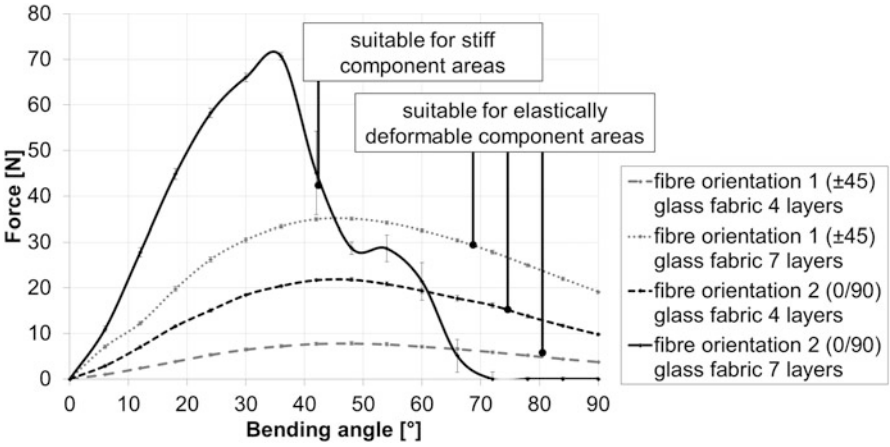

Fig. 9.14 Force-bending angle-diagram: various fibre orientations and laminate thicknesses, respectively

were analysed by Differential Scanning Calorimetry (DSC) to determine their glass transition point. The chosen resin fulfils the temperature requirements for outer façades, i.e. a glass transition temperature of a minimum of 80 °C. Additionally, the bending properties were tested by using a modified two-point-bending test based on DIN 53121 with regard to the curved folding movement. With respect to the established material and stiffness derived from gradients, which were derived from digital simulations concerning the different stiffness gradients within the component, various resin-fibre combinations, laminate thicknesses, fibre materials, fibre orientations and laminate set-ups were tested for their bending behaviour (max. bending angle 90°). An exemplary extract of the test results is given in Fig. 9.14. The tested samples consist of the same resin and the same woven glass fabric. This material combination was tested in two different laminate thicknesses (four and seven layers of fabric) and two different orientations of the fabric.

In Fig. 9.14, the forces necessary to induce various bending angles of the samples are indicated. The curves are based on a sample size of $n = 5$, the dimensions of the samples are 25x50 mm. Unless all samples consist of the same material combination, it is obvious that fibre orientation 2 with a laminate thickness of seven layers leads to a break. In contrast, samples with fibre orientation 1 and a laminate thickness of seven layers stay elastically deformable. In the cases of four-layer-thick laminae, both sample types are elastically deformable but the one with fibre orientation 2 is stiffer and a higher force is needed for bending. The results show that a combination of layers with fibre orientation 1 and 2 enables to achieve defined stiff and elastically deformable areas to be achieved in one component.

The data concerning the mechanical properties were fed back into the simulation to obtain more precise results concerning the possible stiffness range of the used materials and the differentiated fibre orientations. Thus, more information on the

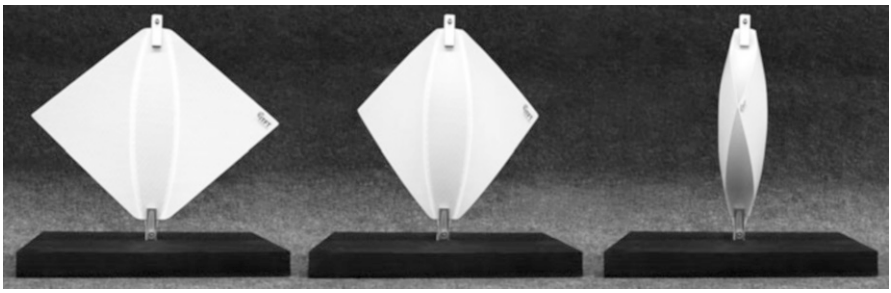

Fig. 9.15 Demonstrator Flectofold

stresses, the required actuation force and the behaviour under external loading can be gained. Eventually, a woven glass fabric was chosen for the building of a first prototype of the Flectofold (Fig. 9.15). By adaption of the fibre orientation and different laminate set-ups within the bending-zone, the backbone and the shading elements, it is possible to implement the *Aldrovanda* curved folding movement principle in the Flectofold demonstrator. In contrast to the biological role model, the backbone of the Flectofold is wider but the bending-zones are narrow. In the bending-zones, the fibres are primarily stressed with shear loads. In the stiffer regions of the Flectofold, as in the backbone and the shading elements, the fibres are stressed both in the fibre and shear direction.

9.5.2 Technical Implementation of Dionaea muscipula's *Trap Movement Principle*

The finding that a mechanical "trick" (snap-buckling) allows the Venus flytrap to snap fast was also beautifully brought into a wider context of physical limits of plant movement (Skotheim and Mahadevan 2005). Although the snap-through transition mechanism has long been widely known among construction engineers and is present, for example, in switches, caps, and even in children's toys, the idea that it is implemented as a plant movement speed-boost feature has resulted in a multitude of papers presenting energy-related and/or motion-related biomimetic applications of this principle (reviewed by Hu and Burgueño 2015; Guo et al. 2015). For example, Holmes and Crosby (2007) have fabricated arrays of micro-lenses, which, by snap-buckling, switch their focal points, Guo et al. (2014) have fine-tuned bistable helical ribbons for shape-shifting, and Lee et al. (2010) have made jumping microgels.

Because of the sudden release of energy and the barely controllable transition between the two stable states (see Sects. 9.2 and 9.4.2), no architectural application is, to our best knowledge, available so far, although the curvature transition from concave to convex offers potential for the geometrical adaptability of façade-shading systems. We believe that investigations into the geometric and mechanical properties

of curvature inversions of doubly-curved shells without snap-buckling, as present in false indusia in *Adiantum* (Poppinga et al. 2015), some *Dionaea* cultivars, e.g. "Korean Melody Shark", and in *Dionaea* trap reopening (Poppinga et al. 2016b), will lead to new insights into the mechanisms at play and inspire transfer to technical structures.

9.6 Discussion and Perspectives

Movements in plants, for example, flower opening and closing, the unfolding of leaves or prey capture movements in carnivorous plants, are highly functional, robust and reliable. In addition, they are typically performed by elastic deformation, i.e. without localised hinges, and have therefore fewer regions of stress concentrations. These features make plant movements especially promising concept generators not only for a novel group of movable structures in architecture, but also for many other applications in various fields of technology, for example, automotive, air- and spacecraft or machine construction. Bioinspired or biomimetic solutions for movable structures in technical applications have the potential to be robust and both disturbance- and maintenance-free, which is of increasing interest for many applications, especially in architecture and building construction (Speck et al. 2016; Knippers and Speck 2012). In addition to these structural and functional features, which are the reasons for the increased interest in bioinspired solutions in building construction and many other field of technology observable during the last few decade(s), an additional feature has to be taken into account in order to understand the specific interest in architecture for bioinspired solutions: a different type of aesthetics based on the beauty of biological movements and functions in general. In the "typically" biomimetic approach, driven by natural scientists, material scientists and engineers, the predictable and reliable transfer of functionalities from the biological role model to the biomimetic product is central, although some of the "aesthetic value" of the biological role model is sometimes lost in this process (Speck 2015). On the other hand, in the art-based process of architectural design, the aesthetic values of biology are often the incentives for choosing a bio-inspired approach (Imhof and Gruber 2015). In the case of bioinspired movable structures, biomimetic products can be developed in which not only the physical functionality is transferred from biology, but additionally a functional elegance similar to that of the highly aesthetic biological role models can be achieved. These cases are still rare and can be considered as the "royal road", i.e. as ideal solutions combining bio-inspired functionality with the natural beauty of function (Speck 2015). The first biomimetic façade-shading system, named Flectofin®, represents such an example. The Flectofin® is a hinge-less resilient biomimetic façade-shading system inspired by the elastic deformation processes taking place during bird pollination on the perch of the Bird-of-paradise flower (*Strelitzia reginae*) (Lienhard et al. 2011; Knippers et al. 2011; Speck et al. 2015). This first successful development combining a "hard approach" to bio-inspired architecture and building construction

(mainly driven by civil engineers, materials scientists and natural scientists) with a "soft approach" to bio-inspired architecture (mainly driven by artists, designers and architects) shows the great potential of biomimetic elastic architecture and allows a promising outlook, especially for bioinspired movable structures.

Acknowledgements We thank Anja and Holger Hennern for their kind permission to include Fig. 9.1c in this chapter. This work has been funded by the German Research Foundation (DFG) as part of the Transregional Collaborative Research Centre (SFB/Transregio) 141'Biological Design and Integrative Structures'/project A04.

References

Antkowiak B, Mayer WE, Engelmann W (1991) Oscillations of the membrane potential of pulvinar motor cells in situ in relation to leaflet movements of *Desmodium motorium*. J Exp Bot 42:901–910

Ashida J (1934) Studies on the leaf movement of *Aldrovanda vesiculosa* L. I. Process and mechanism of the movement. Mem Coll Sci Kyoto Imp Univ Ser B9:141–244

Bailey T, McPherson S (2012) *Dionaea*. The Venus's Flytrap. Redfern Natural History Productions, Poole

Böhm J, Scherzer S, Krol E et al (2016) The Venus flytrap *Dionaea muscipula* counts prey-induced action potentials to induce sodium uptake. Curr Biol 26:1–10

Braam J (2005) Plant responses to mechanical stimuli. New Phytol 165:373–389

Burgert I (2006) Exploring the micromechanics of plant cell walls. Am J Bot 93:1391–1401

Burgert I, Fratzl P (2009) Actuation systems in plants as prototypes for bioinspired devices. Phil Trans R Soc A 367:1541–1557

Campbell NA, Garber RC (1980) Vacuolar reorganization in the motor cells of *Albizzia* during leaf movement. Planta 148:251–255

Colombani M, Forterre Y (2011) Biomechanics of rapid movements in plants: poroelastic measurements at the cell scale. Comput Method Biomec 14:115–117

Cross A (2012) *Aldrovanda*. The Waterwheel Plant. Redfern Natural History Productions, Poole

Darwin C (1865) On the movements and habits of climbing plants. Bot J Linn Soc 9:1–18

Darwin C (1875) Insectivorous plants. Murray, London

Dawson C, Vincent JFV, Rocca AM (1997) How pine cones open. Nature 390:668

Deegan RD (2012) Finessing the fracture energy barrier in ballistic seed dispersal. Proc Natl Acad Sci U S A 109:5166–5169

Dumais J, Forterre Y (2012) "Vegetable dynamicks": the role of water in plant movements. Annu Rev Fluid Mech 44:453–478

Forterre Y (2013) Slow, fast and furious: understanding the physics of plant movements. J Exp Bot 64:4745–4760

Forterre Y, Skotheim JM, Dumais J et al (2005) How the Venus flytrap snaps. Nature 433:421–542

Ge ZW, Yang ZL, Vellinga EC (2010) The genus *Macrolepiota* (Agaricaceae, Basidiomycota) in China. Fungal Divers 45:81–98

Gerbode SJ, Puzey JR, McCormick AG et al (2012) How the cucumber tendril coils and overwinds. Science 337:1087–1091

Guo Q, Zheng H, Chen W et al (2014) Modeling bistable behaviors in morphing structures through finite element simulations. Bio Med Mater Eng 24:557–562

Guo Q, Dai E, Han X et al (2015) Fast nastic motion of plants and bioinspired structures. J R Soc Interface 12:20150598

Henning F (2011) Handbuch Leichtbau. Carl Hanser Verlag, München

Heslop-Harrison Y (1970) Scanning electron microscopy of fresh leaves of *Pinguicula*. Science 167:172–174

Hodick D, Sievers A (1989) On the mechanism of trap closure of Venus flytrap (*Dionaea muscipula* Ellis). Planta 179:32–42

Holmes DP, Crosby AJ (2007) Snapping surfaces. Adv Mater 19:3589–3593

Hovenkamp PH, van der Ham RWJM, van Uffelen GA et al (2009) Spore movement driven by the spore wall in an eusporangiate fern. Grana 48:122–127

Howell LL (2001) Compliant mechanisms. Wiley, New York

Hu N, Burgueño R (2015) Buckling-induced smart applications: recent advances and trends. Smart Mater Struct 24:063001

Imhof B, Gruber P (eds) (2015) Built to grow – blending architecture and biology. Birkhäuser Verlag, Basel

Keijzer CJ, Hoek IHS, Willemse MTM (1987) The processes of anther dehiscence and pollen dispersal. III. The dehydration of the filament tip and the anther in three monocotyledonous species. New Phytol 106:281–287

Knippers J, Lienhard J, Schleicher S et al (2011) Gelenkloser, stufenlos verformbarer Klapp-mechanismus (Hingeless, infinitely deformable folding mechanism). Eur Patent Off Filing 10013852(8)

Knippers J, Speck T (2012) Design and construction principles in nature and architecture. Bioinspir Biomim 7:015002

Knippers J, Scheible F, Oppe M et al (2012) Bio-inspirierte kinetische Fassade für den Themen-pavillon One Ocean Expo 2012 in Yeosu, Korea. Bautechnik 90:341–347

Kobayashi H, Kresling B, Vincent JFV (1998) The geometry of unfolding tree leaves. Proc Roy Soc B 265:147–154

Lee H, Xia C, Fang NX (2010) First jump of microgel; actuation speed enhancement by elastic instability. Soft Matter 6:4342–4345

Liang H, Mahadevan L (2011) Growth, geometry, and mechanics of a blooming lily. Proc Natl Acad Sci USA 108:5516–5521

Lienhard J, Schleicher S, Poppinga S et al (2011) Flectofin: a hinge-less flapping mechanism inspired by nature. Bioinspir Biomim 6:045001

Mitani J, Iagarshi T (2011) Interactive design of planar curved folding by reflection. In: Pacific conference on computer graphics and applications, Kaohsiung, Taiwan, 21–23 September 2011

Müller L (1933) Über den Bau und die Entwicklung des Bewegungsmechanismus von *Physostegia virginiana*. Planta 18:651–663

Nakamura Y, Reichelt M, Mayer VE et al (2013) Jasmonates trigger preyinduced formation of 'outer stomach' in carnivorous sundew plants. Proc Roy Soc B 280:20130228

Niklas KJ (1992) Plant biomechanics: an engineering approach to plant form and function. The University of Chicago Press, Chicago

Peakall R (1990) Responses of male *Zaspilothynnus trilobatus* Turner wasps to females and the sexually deceptive orchid it pollinates. Funct Ecol 4:159–167

Poppinga S, Joyeux M (2011) Different mechanics of snap-trapping in the two closely related carnivorous plants *Dionaea muscipula* and *Aldrovanda vesiculosa*. Phys Rev E 84:041928

Poppinga S, Masselter T, Speck T (2013) Faster than their prey: new insights into the rapid movements of active carnivorous plants traps. BioEssays 35:649–657

Poppinga S, Haushahn T, Warnke M et al (2015) Sporangium exposure and spore release in the Peruvian maidenhair fern (*Adiantum peruvianum*, Pteridaceae). PLoS One 10:e0138495

Poppinga S, Weisskopf C, Westermeier AS et al (2016a) Fastest predators in the plant kingdom: functional morphology and biomechanics of suction traps found in the largest genus of carnivorous plants. AoB PLANTS 8:plv140

Poppinga S, Kampowski T, Metzger A et al. (2016b) Comparative kinematical analyses of Venus flytrap (*Dionaea muscipula*) snap-traps. Beilstein J Nanotechnol 7:664–674

Reith M, Claßen-Bockhoff R, Speck T (2006) Biomechanics in *Salvia* flowers, the role of lever and flower tube in specialization on pollinators. In: Herrel A, Speck T, Rowe N (eds) Ecology and biomechanics: a mechanical approach to the ecology of animals and plants. CRC Press, Boca Raton, pp 123–146

Reith M, Baumann G, Claßen-Bockhoff R et al (2007) New insights in the functional morphology of the lever mechanism of *Salvia pratensis* (Lamiaceae). Ann Bot 100:393–400

Schleicher S (2015) Bio-inspired compliant mechanisms for architectural design. Transferring bending & folding principles of plant leaves. to flexible kinetic structures. Dissertation thesis, University of Stuttgart

Schleicher S, Lienhard J, Poppinga S et al (2015) A methodology for transferring principles of plant movements to elastic systems in architecture. Comput Aided Des 60:105–117

Schürmann H (2007) Konstruieren mir Faser-Kunststoff-Verbunden. Springer, Berlin/Heidelberg

Skead CJ (1975) Weaverbird pollination of *Strelitzia reginae*. Ostrich 46:83–185

Skotheim JM, Mahadevan L (2005) Physical limits and design principles for plant and fungal movements. Science 308:1308–1310

Speck O, Speck D, Horn R, et al (2016) Biomimetic - bio-inspired - biomorph - sustainable? An attempt to classify and clarify biology-derived technical developments. Bioinspir Biomim (accepted)

Speck T, Speck O (2008) Process sequences in biomimetic research. In: Brebbia CA (ed) Design and nature IV. WIT Press, Southampton, pp 3–11

Speck T (2015) Approaches to bio-inspiration in novel architecture. In: Imhof B, Gruber P (eds) Built to grow – blending architecture and biology. Birkhäuser Verlag, Basel, pp 145–149

Speck T, Knippers J, Speck O (2015) Self-x-materials and -structures in nature and technology: bio-inspiration as driving force for technical innovation. Archit Design 85:34–39

Tachi T (2009) Simulation of rigid origami. In: Lang R, Peters AK (eds) Origami 4: the fourth international conference on origami in science, mathematics, and education, vol 4. A K Peters Limited, Natick, pp 175–187

van der Cingel NA (2001) An atlas of orchid pollination. A A Balkema, Rotterdam

van Doorn WG, van Meeteren U (2003) Flower opening and closure: a review. J Exp Bot 54:1801–1812

van Doorn WG, Kamdee C (2014) Flower opening and closure: an update. J Exp Bot 65:5749–5757

Velasco R, Brakke AP, Chavarro D (2015) Dynamic façades and computation: towards an inclusive categorization of high performance kinetic façade systems. In: Celani G, Sperling DM, Franco JMS (eds) Computer-aided architectural design futures. The next city, vol 527, New technologies and the future of the built environment. Springer, Berlin/Heidelberg, pp 172–191

Vincent O, Weißkopf C, Poppinga S et al (2011) Ultra-fast underwater suction traps. Proc Roy Soc B 278:2909–2914

Weintraub M (1952) Leaf movements in *Mimosa pudica* L. New Phytol 50:357–582

Williams SE, Bennett AB (1982) Leaf closure in the Venus flytrap: an acid growth response. Science 218:1120–1122

Williams SE, Pickard BG (1979) The role of action potentials in the control of capture movements of *Drosera* and *Dionaea*. In: Skoog F (ed) Plant growth substances 1979 – Proceedings of the 10th international conference on plant growth substances. Madison, Wisconsin, pp 470–480